Flux-lattice noise and symmetry breaking in frustrated Josephson-junction arrays

N. Grønbech-Jensen,* A. R. Bishop, F. Falo,† and P. S. Lomdahl
Theoretical Division and Advanced Computing Laboratory, Los Alamos National Laboratory, Los Alamos, New Mexico 87545
(Received 28 May 1992)

Long-time dynamics simulations of large (128×128) two-dimensional arrays of Josephson junctions in a uniformly frustrating external magnetic field are reported. The results demonstrate (i) a noisy *transverse* voltage response to an applied current, and (ii) the dependence of the noise on both positional disorder and intrinsic dynamical symmetry breaking induced by boundaries as nucleation sites for flux-lattice defects, which propagate into the interior and control the noise characteristics.

Arrays of Josephson junctions (JJA) provide an excellent controlled laboratory[1] in which to study effects of extended nonlinear dynamical systems: space-time chaos, coherence, pattern formation, etc.[1-3] In this work we take advantage of recent advances in large-scale, long-time Langevin dynamics simulation capabilities[2] to study *noisy* (i.e., multitime-scale) voltage responses, and their relation to multilength scales, in current driven JJA's in the presence of a uniform extended magnetic field which frustrates the flux order. We find noisy voltage responses around a "stick-slip"-type threshold for flux flow, providing an explicit example of self-organized criticality[4] in space-time.

$1/f$ noise has become interesting in high-temperature and conventional superconductors recently because of observations[5] in SQUID's. It has been interpreted variously in terms of "flux-bundle" dynamics or more microscopically in terms of the influence of quasiparticle or conductance fluctuations.[6] Our emphasis here, for JJA's, is in terms of the dynamics of flux *defects* (defined with respect to a ground-state flux order), and, in particular, the influence of symmetry breaking from boundary conditions. In this way our geometry (see below) provides an example of symmetry breaking in a dynamical system, as studied by symmetry group analysis in other extended dynamical systems such as convection cells.[7] We find that our boundary conditions may induce symmetry breaking through intrinsic dynamics in a noisy regime. Furthermore, we find that the symmetry breaking occurs through flux defects which nucleate *at* the boundaries and then propagate into the sample interior, providing macroscopic noise. This is again similar to phenomena observed in other extended dynamical systems, e.g., turbulent fluid regimes,[8] but here we report that the symmetry breaking causes a transverse voltage response to the applied current.

The Hamiltonian for the JJA takes the form[1-3]

$$\mathcal{H}=-E_0\sum_{i,j}[\cos(\theta_{ij}-\theta_{i-1j}-A_{i-1j,ij})+\cos(\theta_{ij}-\theta_{ij-1}-A_{ij-1,ij})]-E_1\sum_j(\theta_{1j}-\theta_{Nj})\ , \tag{1}$$

where θ_{ij} is the phase of the superconducting island with the discrete coordinates (i,j) $[(i,j)\in[1,N]\times[1,N]]$ of the lattice, and $A_{ij,kl}\equiv(2e/\hbar c)\int_{ij}^{kl}\mathbf{A}\cdot d\mathbf{l}$ is the integral of the vector potential from island ij to a neighboring island kl [see also Eq. (4)]. The critical current of the superconducting islands is given by $I_0=(2e/\hbar)E_0$ and the applied current forced through the boundary conditions is given by $I_1=(2e/\hbar)E_1$. The $A_{ij,kl}$ summed around a plaquette obeys the following relation:

$$A_{ij,kl}+A_{kl,kl-1}+A_{k-1l-1,ij-1}+A_{ij-1,ij}=2\pi f\ ,$$

where the frustration $f=Ha^2/\Phi_0$ is a constant giving the average number of flux quanta $\Phi_0=hc/2e$ of the external magnetic field H through the area a^2 of each plaquette of the array. We also introduce[2,9] the fractional charge q_{ij}, obtained as the gauge-invariant phase sum around the ijth plaquette:

$$\begin{aligned}q_{ij}=\frac{1}{2\pi}[&(\theta_{ij}-\theta_{ij-1}-A_{ij-1,ij})\bmod\pi\\&+(\theta_{ij-1}-\theta_{i-1j-1}-A_{i-1j-1,ij-1})\bmod\pi\\&+(\theta_{i-1j-1}-\theta_{i-1j}-A_{i-1j,i-1j-1})\bmod\pi\\&+(\theta_{i-1j}-\theta_{ij}-A_{ij,i-1j})\bmod\pi]\ .\end{aligned} \tag{2}$$

Two situations are discussed in detail below: (a) $f=\frac{1}{2}$ uniformly [in this case $q_{ij}=\pm\frac{1}{2}$, forming a checkerboard ground state, and thus it is sometimes convenient to introduce the staggered order parameter $\tilde{q}_{ij}=(-1)^{(i+j)}q_{ij}$]; (b) $f=\frac{1}{2}$ with static Gaussian disorder[10] of the positions of the superconducting islands.

The dynamical equation for the quantum-mechanical phases takes the form, in the resistively shunted junction (RSJ) model,[2]

$$\begin{aligned}\ddot{\theta}_{ij}=&\sin(\theta_{ij+1}-\theta_{ij}-A_{ij,ij+1})+\sin(\theta_{ij-1}-\theta_{ij}-A_{ij,ij-1})+\sin(\theta_{i+1j}-\theta_{ij}-A_{ij,i+1j})\\&+\sin(\theta_{i-1j}-\theta_{ij}-A_{ij,i-1j})-\eta(\dot{\theta}_{ij+1}+\dot{\theta}_{ij-1}+\dot{\theta}_{i+1j}+\dot{\theta}_{i-1j}-4\dot{\theta}_{ij})+J_1(\delta_{1j}-\delta_{Nj})\ ,\end{aligned} \tag{3}$$

where $\delta_{ij}=1$ for $i=j$ and $\delta_{ij}=0$ for $i\neq j$. Time is normalized to $\tau=(C_0\hbar/2eI_0)^{1/2}$, the normalized dissipation is given by $\eta=(1/R)(\hbar/2eC_0I_0)^{1/2}$ with R the normal resistance of the junctions, and C_0 is the capacitance between a superconducting island and the ground plane. Finally, the normalized bias current is given by $J_1=I_1/I_0$ and voltage is normalized to $\hbar/2e\tau$. As explained in Ref. 2, this choice is appropriate for model *lo-*

cal capacitance coupling of each superconducting island. Temperature can also be introduced, in a classical Langevin sense, as explained in Ref. 2.

The results reported here are restricted to $\eta=5$ (overdamped dynamics), and *uniform* dc current driving along two edges of the array. *Open* boundary conditions are used on *all* edges—this is in contrast to our earlier study[2] where periodic boundary conditions were introduced on the two undriven edges. We also study only the maximal frustration case: $f=\frac{1}{2}$ uniformly throughout the array. The array size is given by $N=128$, making the frustration commensurate. In addition, there are no edge effects other than via the boundary conditions. For details about the numerical method of integration, see Ref. 2. In all our simulations, we have followed the system in 40 000 normalized time units and the integration step size has been varied in order to secure numerical convergence.

Throughout the regimes outlined in Ref. 2, the periodic boundary conditions on the undriven edges of the array, with uniform driving at the other edges, lead to perfect one-dimensional (1d) responses, i.e., uniform flux distributions in the y direction. This symmetry is, of course, broken if thermal noise is applied,[2] but we report here that it can also be broken by the dynamics if the boundary conditions are changed from periodic to open. This represents a striking example of the role of symmetry and boundary conditions on space-time dynamical responses—as observed in other finite extended dynamical systems, e.g., fluid turbulence,[8] where the role of boundaries and boundary layers as nucleation sites for space-time defects, which eventually dominate macroscopic responses.

Figure 1 shows the V-J_1 characteristic with uniform edge driving (at the vertical edges) for all-open boundary conditions. The voltages are here defined by

$$V_x=N_y^{-1}\sum_{j=1}^{N_y}(\dot{\theta}_{N_x j}-\dot{\theta}_{1j})$$

and

$$V_y=N_x^{-1}\sum_{i=1}^{N_x}(\dot{\theta}_{iN_y}-\dot{\theta}_{i1})\ .$$

We see little difference from periodic boundary conditions[2] at this macroscopic level, with the normalized critical current of $J_c\approx 0.35$. Examination of the noise spectrum $S_{V_x}(\omega)$, shown in Figs. 2(a) and 2(b), reveals the presence of a window of *noisy* response for $J_c(f=\frac{1}{2})\leq J_1\lesssim 0.55$. This multitime-scale response is understood[2] in terms of irregular domain-wall separations, shown in the staggered charge $\bar{q}_{ij}$ plot representation of the insets in Fig. 1. Figure 1(b) shows that a *large transverse* voltage V_y is exclusively associated with the chaotic regime of the driving current. Indeed, we see that the amplitude of V_y is largest in the noisiest driving regime and vanishes (within our numerical resolution) in the regular regimes. Furthermore, the transverse power spectrum $S_{V_y}(\omega)$ supports this scenario: As we see in Fig. 2, the power levels are very similar for V_x and V_y in the noisy regime [Figs. 2(a) and 2(c)], but the noise level is infinitesimal for V_y in the regular regime (not shown), where V_x shows a periodic response [Fig. 2(b)] associated with a regular array of domain walls and uniform injection at the driven edges.

Examination of the $\bar{q}_{ij}$ plots in Fig. 1(a) (insets) clearly demonstrates the nature of the longitudinal symmetry breaking. As shown in the insets of Fig. 1(b), in the regular regime exact symmetry is maintained about the middle of the array ($i=N/2$): thus, V_y for the left and right half arrays *exactly* cancel, even though there is considerable voltage in each half. However, in the noisy regime this left-right symmetry is broken, distinct $\bar{q}_{ij}$ distributions develop [Fig. 1(a)], and the left- and right-half contributions to V_y no longer cancel [Fig. 1(b)], leading to the finite, noisy transverse voltage response shown in Fig. 2(c). Furthermore, as suggested in the $\bar{q}_{ij}$ plots of Fig. 1(a), and as we have observed through careful examination of the time evolution, the asymmetry between left- and right-half planes develops by local flux defects, defined with respect to the domain-wall pattern, nucleat-

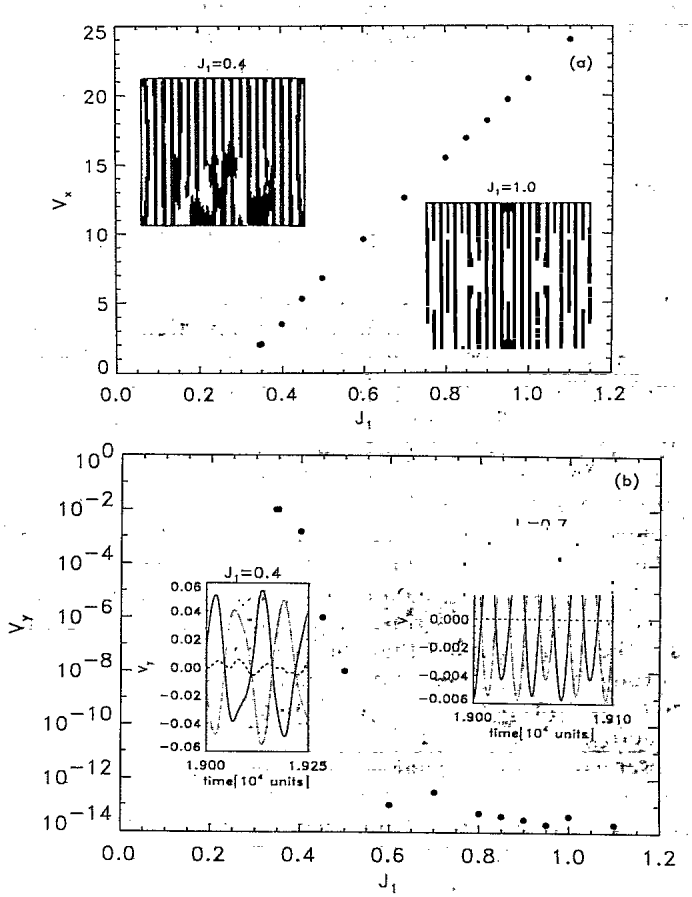

FIG. 1. The dc voltages across the JJA's as a function of the applied bias current J_1: (a) The longitudinal dc voltage V_x vs J_1. Insets show the configuration of $\bar{q}_{ij}$ ($\bar{q}_{ij}>0$, solid; $\bar{q}_{ij}<0$, open) in the cases of two bias currents, $J_1=0.4$ and 1.0. The bias current is forced through the JJA uniformly in the horizontal direction; (b) The amplitude of the transverse ac voltage V_y vs J_1. Insets: time evolution of the transverse voltage V_y (dashed lines) for the cases $J_1=0.4$ and 0.7. Solid curves represent the transverse voltage of the left half of the JJA and the dotted curves represent the transverse voltage across the right half. The solid and the dotted curves add up to the dashed one, which is then the total transverse voltage.

ing (differently) at the upper and lower (undriven) edges and propagating into the interior to form the mesoscopic structures shown in Fig. 1(a).

We have also considered the symmetry-breaking effects of *disorder,* which we introduce as Gaussian positional disorder of the form[10]

$$A_{ij,kl}=2\pi f\frac{x_{ij}+x_{kl}}{2}(y_{kl}-y_{ij}) ,$$
$$x_{ij}=x_{ij}^0+\delta x_{ij},\quad y_{ij}=y_{ij}^0+\delta y_{ij} , \tag{4}$$

where δx_{ij} and δy_{ij} represent the spatial disorder around the ordered positions (x_{ij}^0,y_{ij}^0), $\langle \delta x_{ij}\rangle=\langle \delta x_{ij}\rangle=0$, $\langle \delta x_{ij}\delta x_{kl}\rangle=\langle \delta x_{ij}\delta x_{kl}\rangle=\Delta\delta_{ij,kl}$.

The power levels in the intrinsically noisy regime ($J_c<J_1\lesssim 0.55$) are high and mask effects of the moderate disorder values we consider here (compare Fig. 2 with Figs. 3 and 4). However, in the periodic V_x (zero V_y) regime, $J_1\gtrsim 0.55$, we can systematically observe the symmetry-breaking effects of disorder. Figures 3(a) and 3(b) illustrate how both the noise level and the distribution of time scales increase rapidly in $S_{V_y}(\omega)$ as the disorder strength is increased. The balance between the left and right halves described above is broken giving rise to a finite voltage V_y. However, note that, at small disorder strength [Figs. 3(a) and 4(a)] the frequency distribution

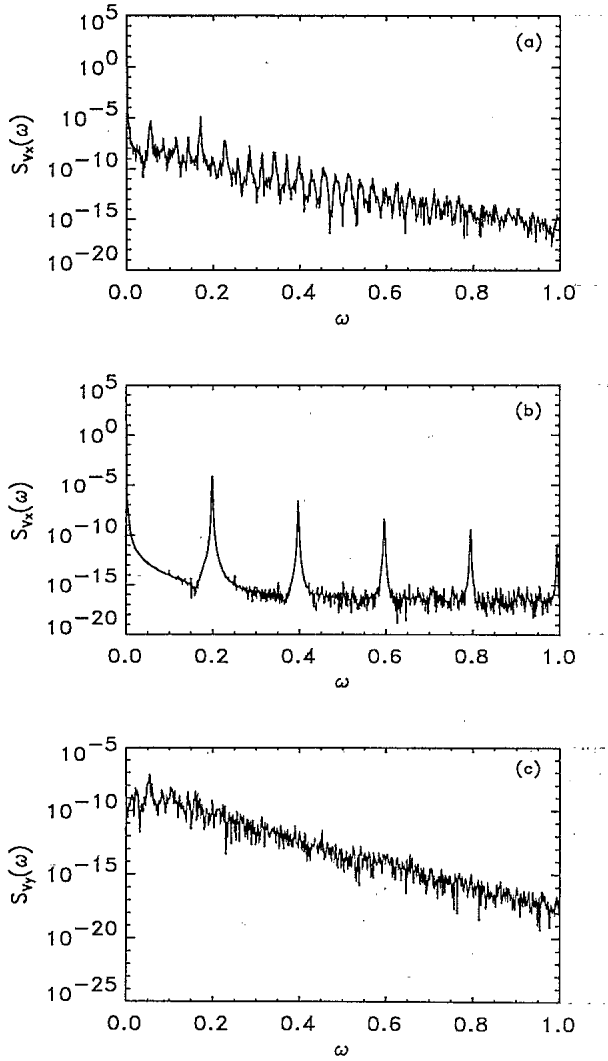

FIG. 2. Spectral densities $S_V(\omega)$ of the voltages: (a) Longitudinal voltage V_x for $J_1=0.4$. (b) Longitudinal voltage V_x for $J_1=0.7$. (c) Transverse voltage V_y for $J_1=0.4$.

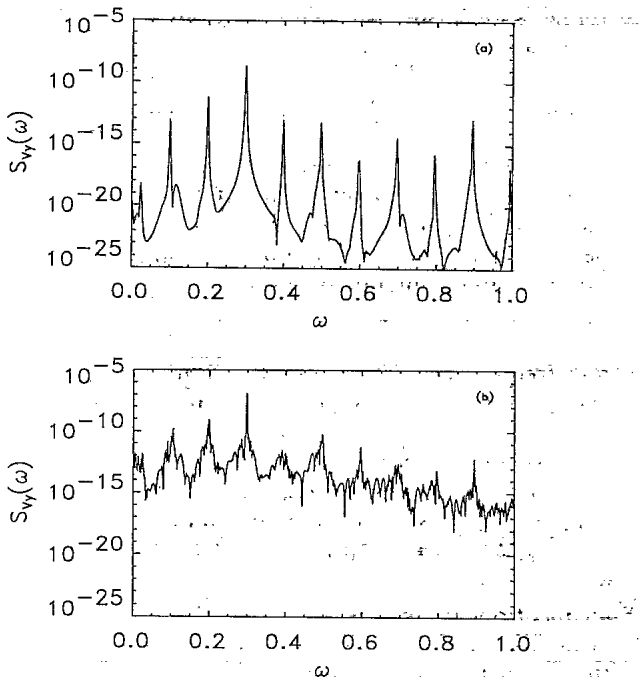

FIG. 3. The spectral densities $S_{V_y}(\omega)$ of the transverse voltages for $J_1=0.7$ when disorder Δ is present (see Fig. 4): (a) $\Delta=0.001$, (b) $\Delta=0.003$.

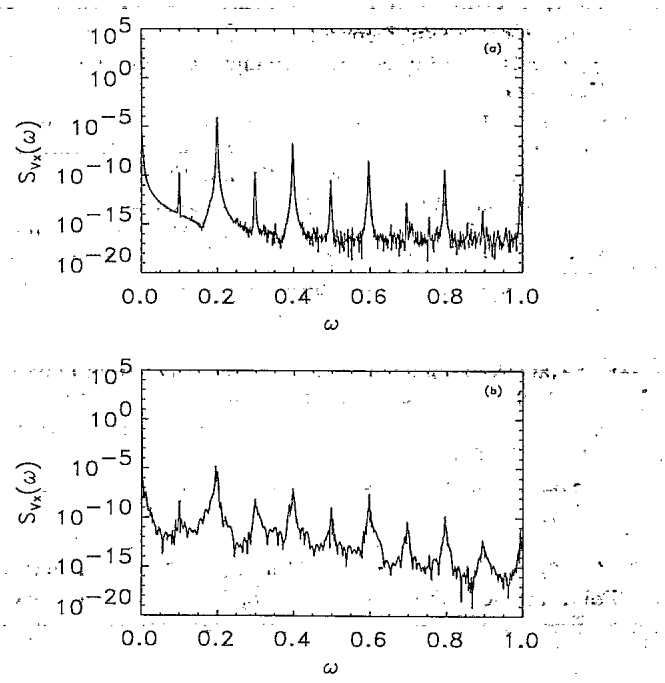

FIG. 4. The spectral densities $S_{V_x}(\omega)$ of the longitudinal voltages for $J_1=0.7$ when disorder Δ is present: (a) $\Delta=0.001$, (b) $\Delta=0.003$.

remains quite smooth. This is because the collective flux structures (which are a result of the intrinsic nonlinearity in the JJA) are able to smooth out the disorder to a weaker effective disorder potential dominated by only a few length scales (and frequencies)—an effect observed in other studies of combined disorder and nonlinearity,[11] and implied in previous simulations of randomly pinned charge-density-wave dynamics.[12] However, as the disorder strength is increased [Figs. 3(b) and 4(b)] many local pinning environments are created for flux structures and collections of structures with the observed consequence of many frequency scales, dressing the dominant lengths and frequencies. The same distribution of flux traps will give rise to Anderson localization, variable range hopping, etc.,[10] at finite temperature.

A second effect of the disorder-induced symmetry breaking is the appearance of *half*-harmonics. This is evident in Fig. 3 for V_y and even more clearly by comparing Fig. 4 with Fig. 2(b) for V_x. The dominant frequency (and harmonics) at $\omega \simeq 0.2$ [see Fig. 2(b)] is due to periodic injection of wall defects from the vertical boundaries. However, the breaking of the left-right symmetry means that each half of the system now contributes separately, which gives the exact subharmonic observed. As we increase the disorder strength [Figs. 3(b) and 4(b)], we again see the multiple frequency scales becoming evident. Here it is interesting to note that a similar type of half-harmonic generation has been found recently for an ac driven system.[13] In that case it was found that the time-varying current drive caused asymmetric vortex-antivortex nucleations in the system and hereby gave rise to half-integer steps in the I-V characteristics.

In summary, we have utilized qualitative advances in our ability to simulate JJA's to (i) illustrate the value of JJA's as an explicit extended dynamical system in which dynamical- and disorder-induced symmetry breaking can result from boundary conditions; (ii) show how defects nucleate at boundaries and result in global space-time noise; and (iii) demonstrate a mechanism for a glassy ($1/f$-like) space-time voltage response due to a frustrated ground state—this can serve as a model for one noise mechanism in real layered superconductors.[5]

We note that JJA's are well within current fabrication capabilities. Although the model studied in this paper has neglected the capacitance of each Josephson link, very preliminary studies show that no qualitative changes arise when this is taken into account. Therefore, we believe that findings of this paper should be possible to verify experimentally.

We thank the Los Alamos Advanced Computing Laboratory for generous support and for making their facilities available to us. N.G.J. is grateful to Otto Mønsteds Fond and to Carlsberg Fondet for financial support during the initial and final parts of this work, respectively. This work was performed under the auspices of the U.S. Department of Energy.

*Permanent address: Department of Applied Physics, Stanford University, Stanford, CA 94305.

†Permanent address: Departamento de Ciencia y Tecnología de Materials y Fluídos, Universidad de Zaragoza–C.S.I.C., Zaragoza, Spain.

[1](a) P. Martinoli, H. Beck, M. Nsabimana, and G. A. Racine, in *Percolation, Localization and Superconductivity,* edited by A. L. Goldman and S. A. Wolf (Plenum, New York, 1984); (b) Ch. Leeman, Ph. Lerch, G.-A. Racine, and P. Martinoli, Phys. Rev. Lett. **56**, 1291 (1986); (c) M. Tinkham and C. J. Lobb, Solid State Phys. **42**, 91 (1989).

[2](a) F. Falo, A. R. Bishop, and P. S. Lomdahl, Phys. Rev. B **41**, 10 983 (1990); (b) N. Grønbech-Jensen, A. R. Bishop, F. Falo, and P. S. Lomdahl, Phys. Rev. B **45**, 10 139 (1992).

[3]For example, K. K. Mon and S. Teitel, Phys. Rev. Lett. **62**, 673 (1989); J. S. Chung, K. H. Lee, and D. Stroud, Phys. Rev. B **40**, 6570 (1989); H. Eikmans and J. E. van Himbergen, *ibid.* **41**, 8927 (1990).

[4]P. Bak, C. Tang, and K. Wiesenfeld, Phys. Rev. Lett. **59**, 381 (1987).

[5]For example, M. J. Ferrari *et al.*, Phys. Rev. Lett. **64**, 72 (1990); W. J. Yeh and Y. H. Kao, Phys. Rev. B **44**, 360 (1991).

[6]For example, Lihong Wang *et al.*, Phys. Rev. Lett. **64**, 3094 (1990).

[7]For example, R. C. Diprima and H. L. Swinney, in *Hydrodynamic Instabilities and the Transition to Turbulence,* edited by J. P. Gollub and H. L. Swinnery (Springer-Verlag, Berlin, 1985); M. Golubitsky, I. Stewart, and D. G. Schaeffer, *Singularities and Groups in Bifurcation Theory* (Springer-Verlag, Berlin, 1988), Vols. I and II.

[8]J. P. Eckmann, G. Goren, and I. Procaccia, Phys. Rev. A **44**, 805 (1991); P. Constantin, I. Procaccia, and K. R. Sreenivasan (unpublished); I. Procaccia *et al.* (unpublished); R. Mehrotra and S. R. Shenoy, Europhys. Lett. **9**, 11 (1989).

[9]See, e.g., T. C. Halsey, Phys. Rev. B **31**, 5728 (1985).

[10]For example, S. P. Benz *et al.*, Phys. Rev. B **38**, 2869 (1988); M. G. Forrester *et al.*, *ibid.* **41**, 8749 (1990); Yin-Hong Li and S. Teitel (unpublished); K. H. Lee and D. Stroud (unpublished); M. P. A. Fisher, T. A. Tokuyasu, and A. P. Young, Phys. Rev. Lett. **66**, 2931 (1991).

[11]R. Scharf and A. R. Bishop, Phys. Rev. A **43**, 6535 (1991).

[12]For example, S. N. Coppersmith and P. B. Littlewood, Phys. Rev. B **31**, 4049 (1985).

[13]D. Dominguez, Jorge V. Jose, and Alain Karma, Phys. Rev. Lett. **67**, 2367 (1991).